

From: FRACTURE MECHANICS OF CERAMICS, Vol. 3
Edited by R. C. Bradt, D. P. H. Hasselman,
and F. F. Lange
(Plenum Publishing Corporation, 1978)

INDENTATION FRACTURE AND STRENGTH DEGRADATION IN CERAMICS

B.R. Lawn and D.B. Marshall

Department of Applied Physics

The University of New South Wales, Australia

ABSTRACT

Brittle ceramic components may suffer severe degradation as a result of localised cracking in contact (notably impact) situations. Such situations, although complicated by a variety of factors, e.g. nature and extent of damage modes operating during the contact, prior state of the exposed surface and the environment, indenter geometry, are most conveniently analysed in terms of "indentation fracture mechanics". This paper accordingly sets out to review the basic principles of indentation fracture and to indicate how these principles may be applied to practical contact problems, with special emphasis on the problem of contact-induced strength loss.

1. INTRODUCTION

Ceramic components in systems exposed to certain unfavorable in-service environments can suffer considerable surface damage from ostensibly minute contact events. Basically, the contacts generate intense stress concentrations, which give rise to characteristic indentation fracture patterns. With the increasing call for ultra-strong materials in high technology it has become more and more necessary to pay attention to the degrading effects that small-scale indenting particles (including liquid drops) may have on mechanical properties. The cumulative effect of a large number of particle contacts can cause rapid erosion and wear of a brittle surface; in structural applications a single contact can reduce the strength of a component by more than an order of magnitude.

"Real" contact situations are very complex. Intuitively, one might expect a large number of variables to enter a general description. Material properties (e.g. toughness, hardness, stiffness), prior state of the brittle surface (e.g. flaw density, level of surface stress), indentation parameters (e.g. indenter geometry, load rate): these are some of the factors which need to be considered. Despite this apparent complexity, a sound basis for classifying and analysing indentation fracture patterns has now been established.¹ Based on whether the contact is essentially elastic ("blunt" indenters) or plastic ("sharp" indenters), the scheme provides a rationale for investigating a wide range of practical problems in ceramics engineering.

In this presentation we survey the basic principles of "indentation fracture mechanics". Our aim is to bring together those results most pertinent to practical applications: details of the formulations have been reviewed elsewhere,¹ and are not included here. In describing geometrical features of the indentation patterns we shall see that certain types of crack tend to penetrate the specimen, and accordingly bear strongly on strength properties, while others tend more to turn back toward the indented surface, and thereby relate more closely to surface-removal properties. Particular attention will be paid here to the question of strength degradation, this lending itself most readily to straightforward analysis in terms of a well-defined indentation crack system.

2. INDENTATION FRACTURE MECHANICS

The experimentation involved in indentation fracture testing is simple. A standard indenter is loaded onto the surface of a test material at a controlled rate, and the attendant crack growth monitored. For general purposes the commercial hardness or crosshead testing machines available in most materials science laboratories are perfectly adequate for delivering the load, and optical techniques applied either during or after indentation usually provide sufficient information on the crack behaviour. More detailed studies may in some cases demand more elaborate equipment,² e.g. environmental chamber, impact apparatus, acoustic sensors (notably for opaque specimens).

What has emerged from comprehensive investigations of indentation fracture patterns on brittle materials, particularly from "model" studies on silicate glasses, is a convenient classification system based on the essential nature of the contact deformation. Indenters are considered "blunt" or "sharp" according to whether the contact is governed by equations of elasticity or plasticity.¹ In their applications to practical

contact fracture situations these two categories may be regarded as limiting cases.

In establishing a theoretical framework for analysing the different types of indentation fracture pattern, one seeks to incorporate the accessible contact parameters into a Griffith-Irwin fracture mechanics formulation.³ First it is necessary to specify the stress field through which the cracks evolve; in this context it is important to appreciate that the general indentation field contains a significant tensile component, even though the loading is ostensibly compressive.⁴ It is the distribution of tensile stresses which ultimately determines the crack driving force and the crack path. A characteristic contact dimension and contact pressure uniquely determine the spatial extent and intensity (i.e. the scale) of the field.

Given the indentation field, one must then ask where and how the cracks initiate. This raises the issue of nucleation centers for the overall fracture process, so the availability of pre-present flaws, either on the surface or in the bulk, becomes an important factor. In a controlled experiment one may choose to regulate the flaw population by a suitable surface abrasion (flaw introduction) or etch (flaw removal) treatment. A simplistic view of the initiation process in the indentation problem is one of providing a precursor energy barrier to full-scale development of the cracks, this being manifested experimentally as a fracture threshold in the applied loading.⁵

Once initiated, the crack propagates in accordance with some extension criterion. It is usual to formulate any such criterion in terms of a convenient fracture mechanics parameter representing the driving force on the crack, e.g. the "crack extension force" G or "stress intensity factor" K .³ Generally, the cracks extend under either equilibrium or kinetic conditions. In the first of these, the critical requirement for extension is determined by a Griffith energy balance expressible as $G_c = K_c^2(1-\nu^2)/E = 2\Gamma$, with Γ the fracture surface energy, K_c the toughness, E Young's modulus and ν Poisson's ratio; equilibrium conditions usually obtain in high vacuum or inert environments, or at low temperatures. In the second case the crack growth is rate controlled, so that a crack velocity requirement $v_c = v_c(K)$ or $v_c(G)$ is applicable; such conditions are met when the fracture takes place in a hostile chemical environment. For a well-defined indentation crack system one then computes an appropriate fracture mechanics function in terms of indentation load P and crack length a , i.e. $K(P, a)$ or $G(P, a)$. This provides sufficient information, in principle, to predict the scale of fracture under any specified loading conditions.

Let us now investigate the different categories of indentation fracture pattern, model and real, in turn. We focus particular attention on crack growth under equilibrium conditions: kinetic effects are regarded as secondary (but by no means unimportant) in the fracture mechanics analysis.

2.1 "Blunt" Indenters

The archetype of the fracture pattern produced under conditions of essentially elastic loading is the classical Hertzian "cone crack". This fracture configuration is most easily obtained with a spherical indenter on a flat specimen surface. Considerable effort has been directed to fracture mechanics studies of cone crack evolution.⁶⁻¹⁴

Figure 1 shows schematically the sequence of events for one complete indentation cycle. The form of the tensile field, with degree of shading representing level of stress, is indicated in diag. (a). While all stress components directly below the elastic contact area are compressive, as one might expect, elsewhere the major principal stress becomes tensile. The tension is particularly strong in a thin, "surface skin" region outside the contact circle. Cone fracture then develops as follows:

(a) the spherical indenter subjects pre-present surface flaws (shown as short dashed lines in diagram) to increasing tensile stress outside the expanding contact circle; (b) upon attaining a critical "Griffith configuration" a favourably located flaw runs around the contact to form a surface "ring crack",⁶ its simultaneous downward growth attenuating to a greater or lesser degree as it extends out of the surface skin region; (c) on further loading, the contact continues to expand and the ring crack is driven downward in controlled fashion, either in equilibrium⁶ or kinetically,¹⁰ deviating outward to avoid the compressive zone; (d) the tension over the area of the crack, although now weak, cumulates with growth in the net driving force until a major instability attains, whence the ring spontaneously develops into a full cone crack (this corresponding to the usually observed critical event in the conventional Hertzian test); (e) on still further loading the crack continues in controlled extension (until the contact circle engulfs the surface ring crack and closes the fracture interface, in which case secondary, tertiary etc. ring cracking may follow); (f) finally, on unloading, the cone crack tries to close and heal to recover the stored elastic energy and surface energy, but is prevented from doing so completely because of mechanical obstruction ("debris", fracture steps, chips, etc.) at the interface¹⁵ (it is for this reason, of course, that the remnant cracks remain visible) - if the unloading is rapid, the

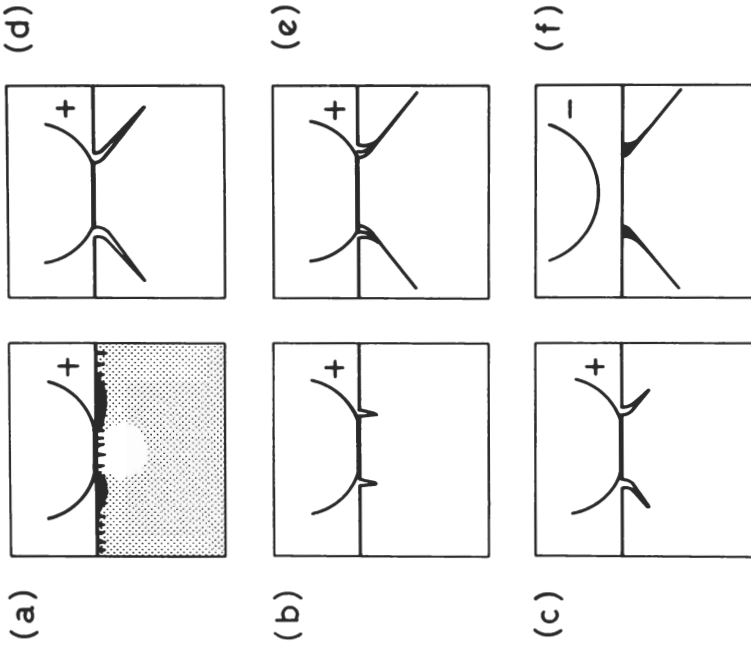


Figure 1: Evolution of cone crack pattern during one complete loading (+) and unloading (-) cycle. Stress field indicated in (a).

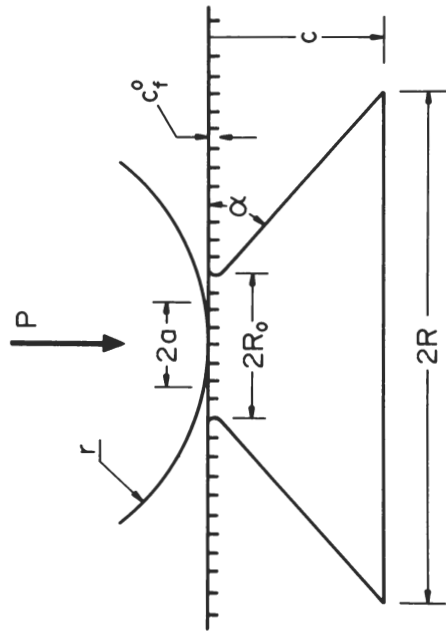


Figure 2: Parameters of Hertzian cone crack system.

base of the cone may turn up in "hat brim" fashion.¹⁶

The indentation parameters used in quantifying the Hertzian fracture process are shown in Figure 2. To establish the scale of the elastic field one resorts to the equations of Hertzian contact.¹⁷ The radius of the contact circle establishes the spatial extent of the field:

$$a = (4kr/3E)^{1/3} P^{1/3} \quad (1)$$

where r is the sphere radius, and $k=(9/16)[(1-\nu^2)+(1-\nu'^2)E/E']$ is a dimensionless constant involving the Young's moduli E , E' , and Poisson's ratios ν , ν' , of specimen and sphere respectively. Likewise, the mean indentation pressure establishes a convenient unit of stress:

$$p_0 = P/\pi a^2 = (3E/4\pi)^{3/2} (kr)^{2/3} P^{1/3} \quad (2)$$

Note that for a given load and sphere size the scale of the field is uniquely determined by elastic constants. In a low-energy impact situation the impulsive load $P(v)$ delivered by a sphere is readily determined from the Hertzian theory, in which case the quantities a and p_0 may equally well be written in terms of impact velocities.^{8,17}

With the application of equilibrium fracture mechanics to the Hertzian configuration one seeks first to specify the threshold conditions under which the cone crack is made to "pop in". On the assumption that the indented surface contains an abundance of large initiating flaws the critical load is found to be⁶

$$P_c = \alpha_E r K_c^2 / E \quad (3)$$

where $\alpha_E = \alpha_E(E/E', \nu)$ is a dimensionless constant of the specimen/indenter materials system. An important conclusion to be drawn here concerns the independence of P_c on the effective initial flaw size σ_f^2 . This is a consequence of the existence of the precursor energy barrier stage (c) in the evolutionary sequence of Figure 1. Equation (3) has been confirmed in a number of experimental studies^{7,8,12,18-21}. The formulation actually breaks down in the limit of small flaws or large spheres,^{6,8} whence the energy barrier diminishes to zero and the cone crack accordingly develops direct from stage (b) to stage (d) in the evolution. It also tends to break down as the flaw density becomes sparse, such that the expanding contact circle has to "search" for a suitable flaw; statistical considerations then enter the problem.¹ Nevertheless, Eqn. (3) remains a useful basis for conservative design in that predictions beyond its range of validity will tend to underestimate in P_c . One drawback is the inability of the theory to predetermine

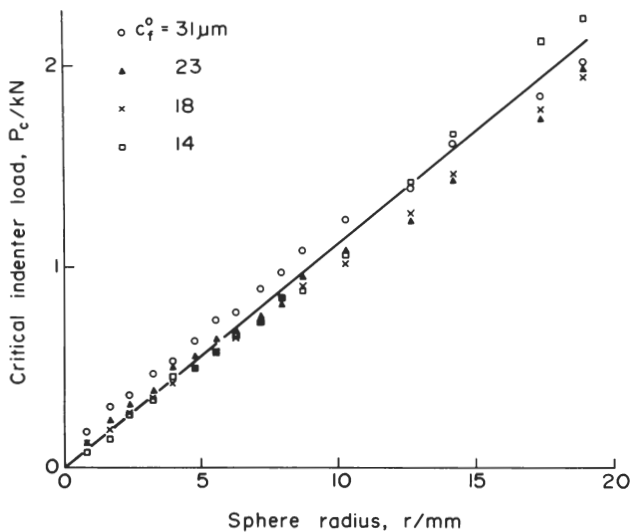


Figure 3: Critical load to cone crack formation as function of sphere indenter radius, steel on soda-lime glass. Glass surfaces pre-abraded to produce controlled flaw population, sizes as indicated. Each point is mean of at least ten tests (standard deviation typically < 10%). Note $P_c \propto r$, but independent of c_f^0 . After Ref. 8.

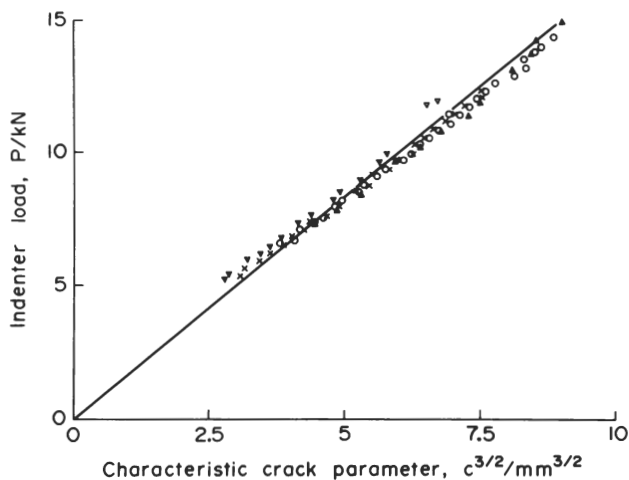


Figure 4: $P(c)$ data for fully-developed cone cracks in soda-lime glass. Truncated sphere indenter. (Measurements made from observations of base radius of cone, using $c=R\tan\alpha$, Fig. 2.) Each symbol represents a separate crack. After Ref. 1.

the constant α_E to much better than an order of magnitude; for this purpose an experimental calibration is desirable. Data in Figure 3 for tests with steel spheres on abraded soda-lime glass surfaces,⁸ in conjunction with independent data on K_C and E for the glass, provide suitable information to effect the calibration, and serve also to highlight the main features of the threshold equation.

Once the cone crack is fully developed, further growth becomes less sensitive to events at the contact zone. The configuration most amenable to fracture mechanics analysis is the limiting one of an ideal cone ($R \gg R_0$), for which one obtains

$$P/c^{3/2} = \beta_E K_C \quad (P > P_c) \quad (4)$$

where $\beta_E = \beta_E(v)$ is a dimensionless constant of the specimen material. This result is seen to be totally insensitive to variations in c_f^0 and α , as one would anticipate from an essentially point-contact configuration. Any errors incurred by neglecting the non-zero surface diameter of the truncated cone in the derivation of Eqn.(4) reflect as overestimates in the predicted crack size, once again consistent with conservative design. The constant β_E is readily calibrated from equilibrium cone crack growth data, such as those for soda-lime glass in Figure 4.

2.2 "Sharp" Indenters

When the contact is essentially plastic* the indenter is deemed to be sharp. Such indenters are typified by the diamond pyramids or cones used in routine hardness testing, although even a sphere is capable of generating precursor plastic flow in less brittle materials.²²⁻²⁴ Evaluation of sharp-indenter fracture mechanics is relatively recent.^{1,4,5,25}

The sequence of events for one complete indentation cycle is shown schematically in Figure 5. In this case the evolution is more complex than for blunt indenters: the elastic/plastic field of the applied loading becomes significantly modified by residual stress effects.²⁶ During the loading half-cycle the tensile field, depicted by shading in diag. (a), peaks directly below the indenter point, where the greatest concentration of deformation and elastic/plastic constraint occurs. This phase of the evolution proceeds in the following way:⁴

* We use the term "plastic" loosely here to include any mode of irreversible deformation, including densification.

(a) the plasticity processes subject sub-surface flaws to a "yield-controlled" level of tensile stress (stresses on pre-present surface flaws being relieved somewhat by the absence of elastic/plastic constraints at the free surface); (b) on the spatial extent of the field reaching some critical level²⁷ one or more of the flaws grow suddenly into sub-surface penny-like cracks, so-called "median cracks", on symmetry planes containing the load axis and major impression diagonals; (c) increased loading expands the contact and drives the median cracks stably downward beneath the indenter and simultaneously upward to intersection with the free surface at the sides, until the geometry tends ultimately to a semicircular profile with linear radial traces extending from the impression corners on the specimen surface (hence an alternative terminology, "radial cracks", although this designation is reserved by some for near-surface, radially directed fractures which are sometimes observed to initiate from particularly large surface flaws^{22, 23}).

Throughout the indentation cycle the stress field is augmented by incompatibility effects at the elastic/plastic interface.²⁶ Thus the field acquires a residual component, and it is the residual stresses which begin to dominate as the indenter is unloaded from the specimen. Diag. (f) in Figure 5 indicates the approximate distribution of residual stresses: most notable is the distortion of the tensile maxima upward toward the free surface. Hence the sequence in the unloading half-cycle:⁴

(d) as unloading starts the walls of the median cracks begin to move together, but fracture debris and residual tension once more prevent total closure (indeed, the residual stresses may actually drive any partially formed median cracks to full development⁵); (e) just prior to full removal of the indenter the residual stresses become sufficient to initiate a completely new system of sideways spreading, saucer-like "lateral cracks"; (f) the lateral cracks continue their spread as the indenter is finally removed, and may actually intersect the free surface to produce a chip²⁸ (growth may persist long after completion of the indentation cycle if the environment is reactive).

Characteristic indentation parameters, such as those shown in Figure 6 for the most widely used Vickers pyramid arrangement, provide the necessary specifications for a fracture mechanics analysis. An idealised sharp-indenter situation invokes the concept of geometrical similarity²⁹ such that the mean contact pressure is invariant with load:

$$p_0 = \text{const.} = H \quad (\text{all } P) \quad (5)$$

where H defines the hardness of the specimen. Then the impression

half-diagonal is given by

$$\alpha = (1/\Lambda\pi H)^{1/2} P^{1/2} \quad (6)$$

for the Vickers geometry of Figure 6 the dimensionless indenter constant Λ is $2/\pi$. It is seen that at a specified load the scale of the field is uniquely determined by plastic properties.

Since the indentation stress field generated during the loading half-cycle is primarily determined by the contact forces, one may reasonably neglect residual stresses in deriving working fracture relations for the median cracks: effects due to the residual component of the field may then be introduced as simple modification factors,³⁰ which may in turn be absorbed into convenient calibration constants in the equations. Starting with the threshold conditions for the formation of the median cracks, again assuming an abundance of large initiating, sub-surface flaws, the critical load is²⁷

$$P_c = \alpha_P K_c^4 / H^3 \quad (7)$$

where $\alpha_P = \alpha_P(v, \text{elastic/plastic zone parameters})$ is a dimensionless constant of the specimen/indenter system. As with its counterpart Eqn. (3) for blunt indenters, Eqn. (7) does not involve the initial flaw size c_f^0 . In this case the computed critical load represents an absolute minimum value for initiation, requiring the presence of an optimal flaw favourably located within the elastic/plastic field; if the density of flaws is sparse such that this requirement is not automatically met, the contact must continue its expansion until a suitable alternative crack source is encountered, whence the value of P_c increases and becomes subject to statistical variations. While Eqn. (7) has not been put to rigorous experimental scrutiny it does bear out empirical findings of higher thresholds in tougher ceramics.²² It would appear that with an appropriate calibration of α_P the equation should serve as an adequate basis for conservative design.

At full development of the median cracks, growth continues with increasing load according to⁵

$$P/c^{3/2} = \beta_P K_c \quad (P > P_c) \quad (8)$$

where $\beta_P = \beta_P(\text{effective indenter angle})$ is a dimensionless constant of the specimen/indenter system. This result is of precisely the same form as Eqn. (4) for well-developed cone cracks: both median and cone cracks extend ultimately on a near-circular front, and accordingly comply with the basic fracture mechanics relations for "penny-like" cracks.⁵ We note again the independence of the result on c_f^0 and α , consistent with the mouth-loading geometry of

Figure 6. Figure 7 shows some median crack data for Vickers pyramid tests on soda-lime glass, from which a calibration value of β_p may be readily determined.

An interesting extension of Eqn. (8) for well-developed median cracks is the case of a biaxially pre-stressed surface, such as in tempered glasses or other ceramics where a residual surface compressive stress σ_R is introduced to oppose fracture. The fracture mechanics relation then modifies to^{31,32}

$$P/c^{3/2} = \beta_p [K_c + \sigma_R (\pi \Omega_c c)^{1/2}] \quad (9)$$

where Ω_c is a dimensionless constant $\approx 4/\pi^2$ for penny cracks of characteristic dimension c . [Comparative measurements of $P(c)$ for the material in its tempered and untempered (control) states accordingly permits an evaluation of σ_R .³²]

Unfortunately, the fracture mechanics of lateral cracking is not so well understood. It will be recalled that lateral cracks develop toward the end of the unloading half-cycle, and thereby associate directly with the residual, elastic/plastic mismatch stress field. The true nature of this field is only beginning to be investigated in a proper analytical way. Several workers have proposed oversimplistic models in which the indentation is viewed in terms of an expanding spherical cavity in an infinite elastic/plastic medium. But such models completely ignore one of the most important features of the lateral crack system, its clear tendency to depart from spherical symmetry in its growth and interact with the free surface. Recent stress field analyses by Perrott²⁶ represent an important first step in incorporating essential surface effects. Empirical observations of lateral crack growth in several ceramics^{22,33} do show the same qualitative trends as for the other crack types in their well-developed form, namely an increase in crack size with peak indentation load.

2.3 "Real" Indenters

How does our analysis of blunt and sharp indenters above help us to understand complex contact events which occur at the surfaces of ceramic structural components during in-service operation? Indenting particles in such situations will generally have a complicated topography of rounded and angular corners and edges, so that the nature of the contact may lie anywhere between the extremes of ideally elastic and ideally plastic. What is more, an indenter of the simplest geometry may act as though blunt in early phases of an indentation cycle, and as sharp in advanced phases of the same cycle.¹ However, none of these complications detract from the present, idealised indentation fracture scheme which takes

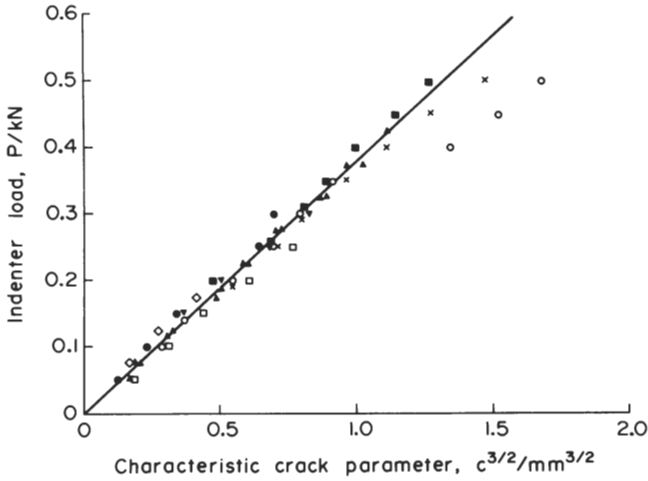


Figure 7: $P(c)$ data for fully-developed median cracks in soda-lime glass. Vickers indenter. Each symbol represents a separate crack. After Ref. 4.

TABLE 1: Essential features of indentation fracture evolution

Blunt Indenters	Sharp Indenters
Initial contact elastic	Initial contact plastic
Tensile component of contact field initiates crack from surface flaw outside contact circle	Tensile component of contact field initiates cracks from subsurface flaw at elastic/plastic interface
Well-developed cone crack extends on circular front	Well-developed median cracks (loading) and lateral cracks (unloading) extend on circular fronts

Figures 1 and 5 as outer bounds to real behaviour.

It is accordingly of some interest to compare and contrast the main features of the fracture mechanics for the blunt and sharp indenter cases. This is done in Table 1. We note that the greatest differences in behaviour occur in the initial stages of contact, where threshold loading is highly sensitive to flaw response in the widely variable near-surface stress field. Generally speaking, the threshold for crack initiation with sharp indenters is some orders of magnitude less than that with blunt indenters. The greatest similarities occur once the indentation cracks have become well developed, since by this stage the fracture geometry is universally penny-like about an effective point-contact center. Thus in applying our blunt/sharp scheme to real contact situations we must expect the indentation fracture predictions to be more reliable at higher loads; of course, it is the severe contact which is of most concern in preventative design.

A complete account of any real contact event may involve any number of variants in fracture behaviour. Our choice of glass as a model brittle material conveniently avoids the factors of microstructure and anisotropy which play such an important role in determining the mechanical properties of most ceramics. These factors, while perhaps not altering the basic mechanisms of indentation fracture, may have an important bearing on the realm of validity of any specific fracture mechanics relation:^{22,23} thus, for instance, striking differences arise in the Hertzian fracture relations for SiO_2 in going from the amorphous form (silica) to the crystalline form (quartz).² Additional variables may enter via velocity effects, either as a result of a reactive environment, whereby subcritical growth can accentuate the fracture,¹ or in high velocity impacts, where dynamic interactions can change the entire nature of the contact field.²³ Friction forces, both in static³⁴ and sliding³⁵ contact, constitute yet a further consideration. In applying the equilibrium equations to any practical contact problem it is important to be aware of the effects of such complicating factors in the prospective damage pattern.

Turning now to practical applications of indentation fracture, we may note that certain of the crack types are likely to assume dominant roles in certain properties. Medians are the most penetrative of all cracks, and are therefore the most dangerous as far as strength is concerned. Lateral cracks conversely interact most strongly with the indented surface, hence relate most closely to erosion and wear. Cone cracks represent an intermediate configuration.

3. CONTACT-INDUCED STRENGTH DEGRADATION

The question of strength degradation lends itself more readily than any other practical problem to indentation fracture analysis. Evans³⁶ was the first to propose a strength theory in terms of formal indentation mechanics, at a time when empirical evidence for the highly deleterious effect of localised contacts on specimen integrity was beginning to mount.³⁷⁻⁴¹ Since the initial work of Evans a comprehensive research program has been initiated to refine and simplify the theory and to determine suitable parameters for design.⁴²⁻⁴⁵

Figure 8 depicts the nature of the problem. In (a) a brittle surface is subjected to an in-service contact event which introduces a penetrant crack of characteristic length c . If the contact is sufficiently severe the indentation crack will constitute the "dominant flaw" in the system. In (b) the surface becomes stressed in tension, most usually by flexure in the case of beam or plate components. The susceptibility to failure from the contact site is then relatively high, and the material is thereby degraded.

The indentation fracture approach to the problem takes as its starting point a standard equation for the strength,

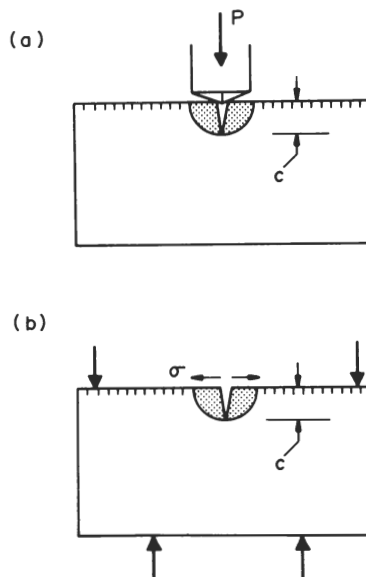


Figure 8: Contact-induced strength degradation: (a) indentation event introduces crack (dominant flaw); (b) subsequent tensile loading (flexure) leads to failure.

$$\sigma = \sigma(c_f), \quad (10)$$

in terms of the effective length c_f of the dominant flaw. In the extreme of light contact loading the size of pre-present flaws will govern the strength, in which case the prior history of the component remains the determining factor. In the opposite extreme of heavy loading c_f identifies with the size of the indentation cracks, whence one may resort to appropriate fracture relations to generate a strength degradation function $\sigma(P)$, or, in an impact situation, $\sigma(v)$, for a given specimen/indenter system. Material fracture parameters then enter the formulation in an explicit and simple way. In this manner one obtains suitable expressions for a priori prediction of strength under any specified loading conditions without the need to resort to extensive strength testing; in principle, the only experimentation that is necessary are "calibration" tests to determine indentation constants (α and β terms, e.g. per Figures 3, 4 and 7) and the material parameters.

In practice, a limited strength testing program is considered desirable to verify essential predictions of the theory. This involves indenting individual specimens, each at a prescribed load, either statically or in impact, and then testing the specimens to failure in a four-point bend test (indented surface on tension side).

To illustrate these ideas we survey the results of studies on two classes of material, those without and with residual surface stresses. Again attention is focussed on equilibrium fracture conditions.

3.1 Non-tempered Materials

Consider an ordinary ceramic material free of any form of surface stress prior to indentation/strength testing. Then the standard strength equation assumes the form

$$\sigma = K_c / (\pi c_f)^{1/2} \quad (11)$$

where c_f is now to be regarded as the effective length of an "equivalent through (straight-edged) crack". The appropriate value of c_f now depends on the relative severity of the indentation-induced crack and pre-present flaws: below some "cutoff load" P^* we have $c_f = c_f^0$, the characteristic size of the pre-present flaws; above P^* we have $c_f = \Omega_c c$, with the dimensionless constant Ω_c a calculable geometrical factor conjugate to the indentation crack depth c . The cutoff load is determined either by the threshold load P_c at which full-scale indentation fracture initiates, or by the crossover load P' at which the condition $\Omega_c c = c_f^0$ is satisfied,

whichever is the greater. Then by recourse to Eqns. (3) and (4) for blunt indenters, or Eqns. (7) and (8) for sharp indenters, one obtains the following strength degradation expressions for general static loading:

$$\sigma = K_c / (\pi c_f^\circ)^{1/2} \quad (P \leq P^*) \quad (12a)$$

$$\sigma = [(\beta K_c^4)^{1/3} / (\pi \Omega_c)^{1/2}] / P^{1/3} \quad (P > P^*) \quad (12b)$$

where we have now dropped subscripts in β . We may expect the degradation function $\sigma(P)$ to exhibit an abrupt discontinuity at P^* when $P_c > P'$, corresponding to the sudden development of a dominant indentation crack. Again, if the impulsive load $P(v)$ in a low-energy impact situation can be evaluated for a given specimen/indenter system, Eqn. (12) can be simply modified to an equivalent degradation function $\sigma(v)$.

Indentation/strength data for soda-lime glass serve to confirm the main features of the theory. In Figure 9 for blunt indenters,^{42,44} and Figure 10 for sharp indenters,⁴³ the curves represent a priori prediction from Eqn. (12) (or, in the impact results, from the corresponding, velocity-modified equation⁴⁴), and the data points represent experiment. The following regions of behaviour may be distinguished:

(i) $P < P^*$; At low loads (or velocities) there is negligible degradation, regardless of the nature of the contact, and prior surface damage controls the strength. In this particular region there is some advantage to be gained by careful surface preparation.

(ii) $P = P^*$; At intermediate loads the strength suddenly declines. The results indicate a very much lower threshold for crack initiation in glass for sharp indenters than for blunt indenters, as one might expect for a geometry of relatively high stress-concentrating power: in Fig. 9 the decline is abrupt, at $P^* = P_c > P'$, whereas in Figure 10 it is smooth, at $P^* = P' > P_c$. In the case of blunt indenters, where the effects of the threshold are manifest, the cutoff is seen to be independent of c_f° , in accordance with Eqn. (3). There is little to be gained by refined surface preparation in this region.

(iii) $P > P^*$; At high loads all strength data asymptotically approach the limiting curve for ideal penny-like indentation cracks. The relatively slight, $P^{-1/3}$ falloff demonstrates a remarkable capacity for structural components to withstand severe contacts (provided the component is not so thin that spontaneous failure conditions are approached during the contact event itself). The remnant strength is now totally independent of c_f° , and indenter geometry enters in an insensitive way through the geometrical terms

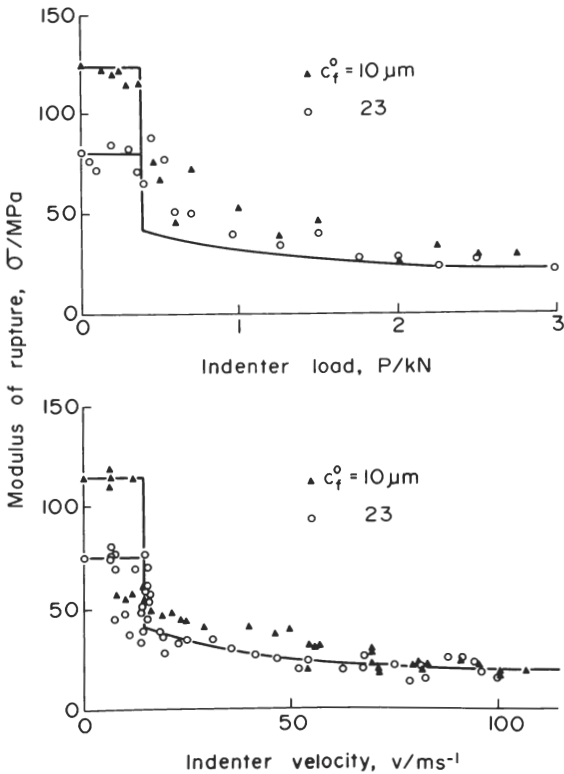


Figure 9: Strength degradation of soda-lime glass, spherical indenters, under conditions of static (top diag., $r=1.6$ mm) and impact (bottom diag., $r=0.8$ mm) loading. Note diminishing effect of abrasion flaw size as severity of loading increases. After Refs. 42 and 44.

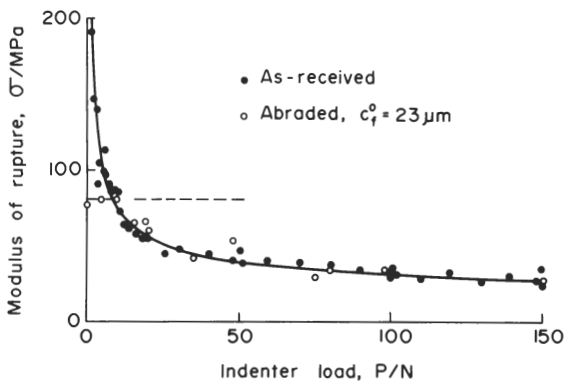


Figure 10: Strength degradation of soda-lime glass, Vickers pyramid indenter, for abraded and as-received surfaces. After Ref. 43.

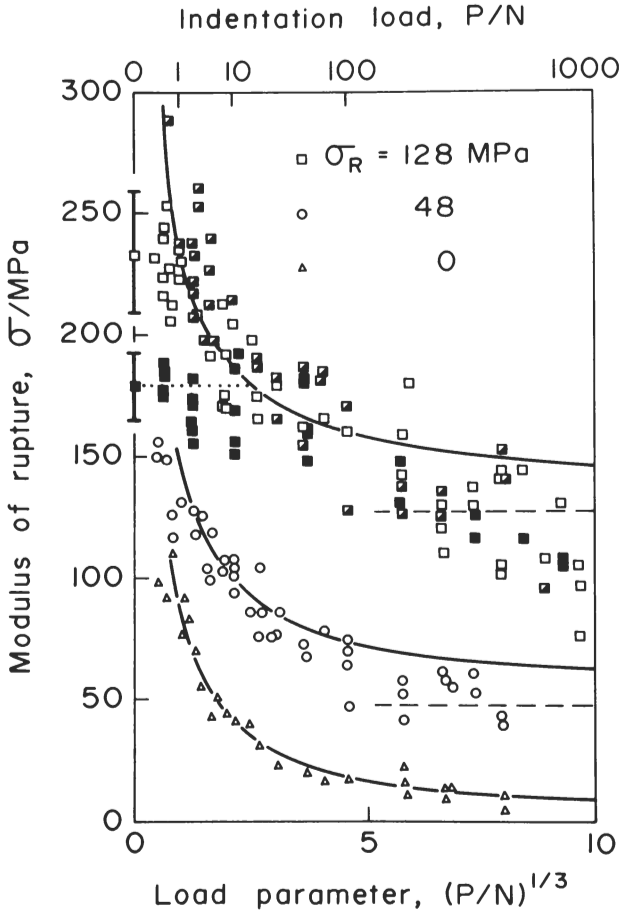


Figure 11: Strength degradation of thermally tempered soda-lime glass, Vickers pyramid indenter. Data for as-received (open symbols), pre-abraded (closed symbols) and pre-etched (half-closed symbols) surfaces. Note significant strengthening with increasing degree of tempering. After Ref. 45.

β and Ω_c in Eqn. (12). An initial state of surface perfection is of no consequence in a general severe contact situation: in this context it is worth recalling (Sect. 2.3) that sharp indenters tend to initiate indentation cracks from sub-surface flaws, and that even ostensibly blunt indenters begin to penetrate and act as though sharp at high load.

3.2 Tempered Materials

It is one thing to be able to predict the resistance to strength degradation for a given material, and quite another to improve it. Surface etching has been generally seen as a means of raising strength, but, as the previous subsection has amply demonstrated, any such gains are more than negated by a single, subsequent contact event. The most practical method available to ceramic materials, especially to glasses, is to put the surfaces in residual compression.^{4 6} This may be done by a variety of physical or chemical "tempering" processes.

Suppose then that a surface subjected to some such tempering process contains a residual compressive stress σ_R . This stress will act biaxially in the surface, but will change and gradually become tensile below the surface toward the inner regions of the plate (in order to satisfy the requirements of zero net force across any section of the specimen). Provided the depth of the dominant flaw is small compared with the characteristic depth of the compression zone, the strength in Eqn. (11) modifies simply to^{4 5}

$$\sigma = K_c / (\pi c_f)^{1/2} + \sigma_R \quad (13)$$

The elimination of c_f from this equation is carried out as before, but with the appropriate indentation fracture relation itself incorporating a residual stress term: thus for sharp indenters, for instance, Eqn. (9) replaces Eqn. (8) in the analysis. Surface compression therefore increases the resistance to degradation on two counts: first, the size of the indentation crack introduced is smaller, for a specified load, Eqn. (9); second, the compression represents a closure stress which has to be overcome before any surface flaw can begin to experience tension in subsequent flexure, Eqn. (13). The strength degradation characteristic $\sigma(P)$ becomes an increasing function of σ_R .

Figure 11 accordingly shows indentation/strength data for thermally tempered soda-lime glass using a sharp indenter.^{4 5} At low loads, $P < P^*$, there is the usual dependence of the strength on prior surface condition. At high loads, $P > P^*$, the curves once again show a steady decline, but now tending asymptotically to

the strength limit σ_R for large flaws in Eqn. (13). (Some "overshoot" in the data fit to the predicted curves occurs at high loads, indicative of departure from the assumption of zero stress gradients in the fracture mechanics.⁴⁵) At all loads the strength of the glass is dramatically improved by the tempering process.

3.3 Implications in Design

The above analysis has certain implications in the design of ceramic components for structural applications. We may summarise these as follows:

- (i) Strength predictions for a given specimen/indenter (target/projectile) system can be made *a priori*; routine, static indentation tests provide the necessary contact coefficients. (In principle, a limited indentation/strength experiment can determine the necessary material constants, and even the residual stress term, as well.⁴⁵) Moreover, the evaluated degradation curves usually (not always) fall below the data points, so the theory tends to be conservative in strength prediction.
- (ii) The classification into blunt and sharp indenters provides upper and lower bounds to the strength characteristics of real contact systems.
- (iii) The formulation is explicit in material parameters, and accordingly provides a sound basis for materials selection. In particular, toughness K_C is the controlling material parameter in the degradation function Eqn. (12), and should be maximised. Stiffness E and hardness H enter only as secondary parameters, through the threshold relations Eqns. (3) and (7): these parameters should be minimised.
- (iv) Contact parameters are important in determining threshold conditions, but diminish in their influence on strength properties at high contact loads. Flaw parameters play an even less significant role in the degradation mechanics.
- (v) Resistance to strength degradation can be substantially improved by introducing compressive stresses into the surface.

4. CONCLUDING REMARKS

This paper has sought to review the theoretical framework of indentation fracture mechanics, and to demonstrate the pertinence of this framework to the strength of materials. We have not dwelt on indentation fracture as a mechanical test in its own right,

with its capacity for providing fundamental information on fracture energies, crack velocities, flaw statistics, etc. in a uniquely simple and economic way. Nor have we given explicit attention to the relevance of contact-induced cracking, notably lateral cracking, to the important surface-removal properties erosion and wear, grinding and abrasion, and comminution. Some of these additional facets of indentation theory have been considered in other review papers,^{1,47} some are addressed elsewhere in this volume, and others remain subjects for future study.

ACKNOWLEDGEMENT

The authors acknowledge the Australian Research Grants Committee for funding of the indentation fracture program at U.N.S.W.

REFERENCES

1. B.R. Lawn and T.R. Wilshaw, "Indentation Fracture: Principles and Applications", *J.Mat.Sci.* 10, 1049 (1975).
2. M.V. Swain, J.S. Williams, B.R. Lawn and J.J.H. Beek, "A Comparative Study of the Fracture of Various Silica Modifications Using the Hertzian Test", *J.Mat.Sci.* 8, 1153 (1973).
3. B.R. Lawn and T.R. Wilshaw, "Fracture of Brittle Solids", Cambridge University Press, Cambridge, 1975. Chs. 3,4,8.
4. B.R. Lawn and M.V. Swain, "Microfracture Beneath Pointed Indentations in Brittle Solids", *J.Mat.Sci.* 10, 113 (1975).
5. B.R. Lawn and E.R. Fuller, "Equilibrium Penny-Like Cracks in Indentation Fracture", *J.Mat.Sci.* 10, 2016 (1975).
6. F.C. Frank and B.R. Lawn, "On the Theory of Hertzian Fracture", *Proc.Roy.Soc.Lond.* A299, 291 (1967).
7. B.R. Lawn, "Hertzian Fracture in Single Crystals with the Diamond Structure", *J.Appl.Phys.* 39, 4828 (1968).
8. F.B. Langitan and B.R. Lawn, "Hertzian Fracture Experiments on Abraded Glass as Definitive Evidence for an Energy Balance Explanation of Auerbach's Law", *J.Appl.Phys.* 40, 4009 (1969).

9. F.B. Langitan and B.R. Lawn, "Effect of a Reactive Environment on the Hertzian Strength of Brittle Solids", J.Appl.Phys. 41, 3357 (1970).
10. A.G. Mikosza and B.R. Lawn, "Section-and-Etch Study of Hertzian Fracture Mechanics", J.Appl.Phys. 42, 5540 (1971).
11. T.R. Wilshaw, "The Hertzian Fracture Test", J.Phys.D.: Appl. Phys. 4, 1567 (1971).
12. J.S. Nadeau, "Hertzian Fracture of Vitreous Carbon", J.Am. Ceram. Soc. 56, 467 (1973).
13. F.C. Roesler, "Brittle Fractures Near Equilibrium", Proc. Phys.Soc.Lond. B69, 981 (1956).
14. M.V. Swain and B.R. Lawn, "A Microprobe Technique for Measuring Slow Crack Velocities in Brittle Solids", Internat.J.Fract. 9, 481 (1973).
15. J.S. Williams, B.R. Lawn and M.V. Swain, "Cone Crack Closure in Brittle Solids", Phys.Stat.Sol.(a) 2, 7 (1970).
16. C.J. Culf, "Fracture of Glass Under Various Liquids and Gases", J.Soc.Glass Tech. 41, 157 (1957).
17. S.P. Timoshenko and J.N. Goodier, "Theory of Elasticity", McGraw-Hill, New York, 1970. Ch. 13.
18. F. Auerbach, "Measurement of Hardness", Ann. Phys.Chem. 43, 61 (1891).
19. F.C. Roesler, "Indentation Hardness of Glass as an Energy Scaling Law", Proc.Phys.Soc.Lond. B69, 55 (1956).
20. J.P.A. Tillet, "Fracture of Glass by Spherical Indenters", Proc.Phys.Soc.Lond. B69, 47 (1956).
21. B.D. Powell and D. Tabor, "The Fracture of Titanium Carbide Under Static and Sliding Contact", J.Phys.D: Appl.Phys. 3, 783 (1970).
22. A.G. Evans and T.R. Wilshaw, "Quasi-Plastic Solid Particle Damage in Brittle Materials: I. Observations and Analysis", Acta Met. 24, 939 (1976).
23. A.G. Evans and T.R. Wilshaw, "Dynamic Solid Particle Damage in Brittle Materials: An Appraisal", J.Mat.Sci. 12, 97 (1977).

24. M.V. Swain, "Indentation Plasticity and the Ensuing Fracture of Glass", J.Phys.D: Appl.Phys. 9, 2201 (1976).
25. B.R. Lawn, T. Jensen and A. Arora, "Brittleness as an Indentation Size Effect", J.Mat.Sci. 11, 573 (1976).
26. C.M. Perrott, "Elastic/Plastic Indentation: Hardness and Fracture", Wear, in press.
27. B.R. Lawn and A.G. Evans, "A Model for Crack Initiation in Elastic/Plastic Indentation Fields", J.Mat.Sci., in press.
28. B.R. Lawn, M.V. Swain and K. Phillips, "On the Mode of Chipping Fracture in Brittle Solids", J.Mat.Sci. 10, 1236 (1975).
29. D. Tabor, "Hardness of Metals", Clarendon Press, Oxford, 1951.
30. J.J. Petrovic, R.A. Dirks, L.A. Jacobson and M.G. Mendiratta, "Effects of Residual Stresses on Fracture from Controlled Surface Flaws", J.Am.Ceram.Soc. 59, 177 (1976).
31. B.R. Lawn and D.B. Marshall, "Contact Fracture Resistance of Physically and Chemically Tempered Glass Plates: A Theoretical Model", Phys.Chem.Glasses 18, 7 (1977).
32. D.B. Marshall and B.R. Lawn, "An Indentation Technique for Measuring Stresses in Tempered Glass Surfaces", J.Am. Ceram.Soc. 60, 86 (1977).
33. M.V. Swain, "Microcracking Associated with the Scratching of Brittle Solids", this volume.
34. K.L. Johnson, J.J. O'Connor and A.C. Woodward, "The Effect of Indenter Elasticity on the Hertzian Fracture of Brittle Materials", Proc.Roy.Soc.Lond. A334, 95 (1973).
35. B.R. Lawn, "Partial Cone Crack Formation in a Brittle Material Loaded with a Sliding Spherical Indenter", Proc.Roy.Soc.Lond. A299, 307 (1967).
36. A.G. Evans, "Strength Degradation by Projectile Impacts", J.Am.Ceram.Soc. 56, 405 (1973).
37. H.P. Kirchner, R.M. Gruver and R.E. Walker, "Strength Effects Resulting from Simple Surface Treatments", in The Science of Ceramic Machining and Surface Finishing, N.B.S. Spec. Publ. 348, 1972. p. 353.

38. R.M. Gruver and H.P. Kirchner, "Effect of Surface Damage on the Strength of Al_2O_3 Ceramics with Compressive Surface Stresses", *J.Am.Ceram.Soc.* 56, 21 (1973).
39. R.M. Gruver and H.P. Kirchner, "Effect of Environment on Penetration of Surface Damage and Remaining Strength of Al_2O_3 ", *J.Am.Ceram.Soc.* 57, 220 (1974).
40. R.M. Gruver and H.P. Kirchner, "Effect of Leached Surface Layers on Impact Damage and Remaining Strength of Silicon Nitride", *J.Am.Ceram.Soc.* 59, 85 (1976).
41. J.J. Petrovic, L.A. Jacobson, P.K. Talty and A.K. Vasudevan, "Controlled Surface Flaws in Hot-Pressed Si_3N_4 ", *J.Am.Ceram.Soc.* 58, 113 (1975).
42. B.R. Lawn, S.M. Wiederhorn and H.H. Johnson, "Strength Degradation of Brittle Surfaces: Blunt Indenters", *J.Am.Ceram.Soc.* 58, 428 (1975).
43. B.R. Lawn, E.R. Fuller and S.M. Wiederhorn, "Strength Degradation of Brittle Surfaces: Sharp Indenters", *J.Am.Ceram.Soc.* 59, 193 (1976).
44. S.M. Wiederhorn and B.R. Lawn, "Strength Degradation of Glass Resulting from Impact with Spheres", *J.Am.Ceram.Soc.*, in press.
45. D.B. Marshall and B.R. Lawn, "Strength Degradation of Thermally Tempered Glass Plates", *J.Am.Ceram.Soc.*, in press.
46. F.M. Ernsberger, "Strength of Brittle Ceramic Materials", *Bull.Am.Ceram.Soc.* 52, 240 (1973).
47. B.R. Lawn and D.B. Marshall, "Mechanisms of Micro-Contact Fracture in Brittle Solids", in proceedings of Conference on Lithic Use-Wear, Simon Fraser University, Canada, to be published.